

# Asteroid rotation and shapes from numerical simulations of gravitational re-accumulation

Paolo Tanga<sup>a,\*</sup>, D. Hestroffer<sup>b</sup>, M. Delbò<sup>a,1</sup>, D.C. Richardson<sup>c</sup>

<sup>a</sup>Laboratoire Cassiopée, UMR CNRS 6202, Observatoire de la Côte d'Azur, BP 4229, 06304 Nice Cedex 04, France

<sup>b</sup>IMCCE, UMR CNRS 8028, Observatoire de Paris, 77 avenue Denfert-Rochereau, F-75014 Paris, France

<sup>c</sup>Department of Astronomy, University of Maryland, College Park, MD 20742, USA

Received 15 January 2008; received in revised form 25 June 2008; accepted 30 June 2008

Available online 23 July 2008

## Abstract

We present simulations of the gravitational collapse of a mono-disperse set of spherical particles for studying shape and spin properties of re-accumulated members of asteroid families. Previous numerical studies have shown that these “gravitational aggregates” exhibit properties similar to granular continuum models described by Mohr–Coulomb theory. A large variety of shapes is thus possible, in principle consistent with the observed population of asteroid shapes.

However, it remains to be verified that the re-accumulation following a catastrophic disruption is capable of naturally producing those shapes. Conversely, we find that fluid equilibrium shapes (flattened two-axis spheroids, in particular) are preferentially created by re-accumulation. This is rather unexpected, since the dynamical system used could allow for other stable configurations. Jacobi three-axial ellipsoids can also be created, but this seems to be a less common outcome.

The results obtained so far seem to underline the importance of other non-disruptive shaping factors during the lifetime of rubble-pile asteroids.

© 2008 Elsevier Ltd. All rights reserved.

*Keywords:* Asteroids; Asteroid formation; Asteroid evolution; Collisions

## 1. Introduction

The currently observable asteroids have been shaped and redistributed by complex dynamical and collisional processes. In particular, “dynamical families” have been identified as groupings in orbital element space, corresponding to ancient destructions of larger parent bodies (Davis et al., 1979; Farinella et al., 1982). This fact is corroborated by the taxonomy of families, whose members also share similar spectroscopic properties.

Over the past several years growing evidence suggests that an important fraction of large family members could be the result of a gravitational re-accumulation of

fragments produced after the parent body disruption (i.e. Michel et al., 2002). As a consequence, these “gravitational aggregates” (also nicknamed “rubble-piles”) would lack any internal cohesion and would have a very low tensile strength.

Gravitational re-accumulation has been modelled recently by numerical simulations employing Smooth Particle Hydrodynamics codes (for the disruption phase) coupled with gravitational N-body codes capable of treating collisions (for the re-accumulation phase). The simulations have also shown that during the gravitational re-accumulation multiple mutually orbiting systems can be created (Michel et al., 2001; Durda et al., 2004).

The low bulk density found for some asteroids, hinting to internal “empty” spaces (high porosity) and the structure of some objects visited by space probes, seem to provide the observational evidence of the existence of gravitational aggregates. We recall here, for example, the low density ( $1.3 \text{ g cm}^{-3}$ ) of (253) Mathilde, about 3 times

\*Corresponding author. Tel.: +33 4 92 00 30 42.

E-mail address: [Paolo.Tanga@oca.eu](mailto:Paolo.Tanga@oca.eu) (P. Tanga).

URL: <http://www.obs-nice.fr/tanga/> (P. Tanga).

<sup>1</sup>Also at INAF, Astronomical Observatory of Torino, Italy. Supported by the European Space Agency (ESA).

smaller than the density of meteorites of supposedly similar composition (Yeomans et al., 1997). Also, Britt et al. (2002) identifies two categories of shattered rubble-piles corresponding to different porosity levels.

However, the search for hints about the rubble-pile nature of asteroids is just starting. Several measurable characteristics are usually tested against the expected properties of such bodies, namely spin rates and shapes. We use these characteristics in our numerical investigations of the origin of these bodies. The conclusion we reach can be considered much more advanced than the very preliminary reports in Consigli et al. (2007) and Tanga et al. (2006).

On the theoretical side, shapes and spins of asteroids are assessed based on the concept of equilibrium shapes of rotating, self-gravitating bodies with low internal cohesion. Hereinafter we will mainly consider the two main paradigms that have been tentatively applied to asteroids, treating them either as perfect fluids (Farinella et al., 1981), or as obeying to the Mohr–Coulomb theory (Holsapple, 2001), appropriate for describing an elastic–plastic behavior for stresses below the yield point. Such material can be considered to be cohesionless, but exhibiting a certain shear strength that prevents it from behaving like a perfect fluid. The typical example on Earth is granular material, such as sand or gravel, that can form conic piles with a well defined maximum slope.

In numerical simulations, the simplest approximation for describing cohesionless rubble-piles is the “perfect rubble pile” (Richardson et al., 2005), represented by self-gravitating, hard spherical particles of equal radii, with no cohesion. Richardson et al. (2005) studied the stability of such bodies starting from a variety of ellipsoidal, rotating aggregates, formed by filling the corresponding hull with closely packed spherical particles. These systems were allowed to evolve under the effect of gravity (using N-body simulations), in order to check their stability or their tendency to readjust to a shape different from the original one.

The results obtained by Richardson et al. (2005) show that a large variety of stable shapes exists in this model, consistent with a Mohr–Coulomb behavior. This good match is due to the macroscopic granular structure of the bodies, which introduces a shear strength. The stable set includes a variety of shapes that could in fact correspond to the observed diversity.

In this work we investigate another part of the story. Namely, we want to check the role of the re-accumulation process, dominated by gravity only, in the generation of shapes. We would like to answer to the following questions: Can all the stable shapes found in Richardson et al. (2005) be generated by re-accumulation? Is gravity alone capable of producing that variety? Which parameters control the final result?

As we will see, a definitive answer cannot yet be given, but we think that some strong hints can already emerged. In the future, we could possibly try to explain some puzzling characteristics of the observed shapes, such as the tendency of the primaries of asteroids with satellites to

cluster close to the fluid equilibrium sequences (Hestroffer, 2004; Hestroffer and Tanga, 2005). Of course, for many re-accumulated asteroids the primitive shapes and spins have been altered by subsequent minor collisions or by other mechanisms. For example, we know that thermal emission can produce a torque capable of changing spin direction and rate (YORP effect). Also, spin around a non-principal axis of a non-rigid body can cause the shape to readjust due to strains during the time of relaxation. We are aware that these processes, which we do not take into account, can be relevant if a comparison to the observed objects is attempted, and their poorly understood nature constitutes a real limitation that should be surmounted in forthcoming explorations.

The paper is organized as follows. In Section 2 we provide an overview concerning observation and theoretical modelling of asteroid shapes, by recalling the theories of fluid equilibrium figures and the Mohr–Coulomb description. In Section 3 we present the numerical method adopted to simulate re-accumulation. The results are presented and discussed in Section 4.

## 2. Asteroid shapes

### 2.1. Equilibrium shapes

Large celestial bodies (with diameters of several thousands of kilometers) should all have their internal strength dominated by gravity on the largest scales. As a consequence, they relax to some equilibrium shape. This is obviously the case for gaseous planets and stars (though inhomogeneity and compressibility are also an issue). The situation is different for asteroids with sizes from kilometers to several hundreds of kilometers. While the original idea of Farinella et al. (1981) was that rubble-pile asteroids could follow figures of equilibrium for fluids, it has been shown that such asteroids could still sustain strains and shapes differing from the hydrostatic equilibrium (Holsapple, 2001). Starting with Newton, figures of equilibrium for incompressible fluids have been studied by numerous mathematicians and astronomers, including Maclaurin, Clairaut, Jacobi, Darwin, Poincaré, Liapunov, Jeans, Chandrasekhar, Kopal, Tassoul, etc.

The theory of equilibrium shapes has been thoroughly described in several papers, from the classic work Chandrasekhar (1969) to extensions relevant for asteroids such as Lai et al. (1993); Hachisu and Eriguchi (1984), therefore we will not address the whole issue here again. For sake of clarity and interpretation of results, however, it is worth recalling some basic concepts.

The approach is to consider self-gravitating fluid bodies, whose equilibrium figures are described—in a cartesian system aligned with the body axes and centered on the body—in terms of ellipsoids defined as

$$\left(\frac{x}{a}\right)^2 + \left(\frac{y}{b}\right)^2 + \left(\frac{z}{c}\right)^2 = R^2, \quad (1)$$

where  $a$ ,  $b$  and  $c$  represent the ellipsoid semi-axes, and  $R$  the radius of a mass-equivalent sphere. The use of adimensional quantities greatly facilitates the task of shape parametrization, since the dependence on particular choices such as the values of  $R$  or the density is eliminated. Hereinafter, we thus make use of the axis ratios ( $b/a, c/a$ ), and we normalize the spin  $\Omega$  and angular momentum  $L$ , respectively, as  $\bar{\Omega} = \Omega/(\pi G\rho)^{1/2}$  and  $\bar{L} = L/(Gm^3 R)$ .

The stability solutions for incompressible fluids are the classical results (Chandrasekhar, 1969) and show that for low rotation rates a “sequence” of flattened spheroids with  $a = b$  (Maclaurin sequence) exists. Along this sequence, the flattening  $e = \sqrt{1 - (c/a)^2}$  is related to the normalized spin by

$$\bar{\Omega} = 2(3 - 2e^2) \frac{\sqrt{1 - e^2}}{e^3} \arcsin(e) - \frac{6(1 - e^2)}{e^2}. \quad (2)$$

Also, the following relation holds:

$$\bar{L} = \frac{\sqrt{3}}{5} \left(\frac{a}{R}\right)^2 \bar{\Omega}. \quad (3)$$

It has been demonstrated that bodies belonging to this sequence are secularly stable for increasing  $\bar{L}$  values up to  $\bar{L}_{c1} = 0.304$ . Higher angular momentum bodies tend to accommodate along another set of solutions, corresponding to a sequence of three-axial ellipsoids (the Jacobi sequence) characterized by a smaller spin rate. For the Jacobi sequence similar relations are found:

$$\bar{\Omega} = 2abc \int_0^{+\infty} \frac{u du}{(a^2 + u)(b^2 + u)\Delta}, \quad (4)$$

$$\Delta^2 = (a^2 + u)(b^2 + u)(c^2 + u) \quad (5)$$

and

$$\bar{L} = \frac{\sqrt{3}}{10} \frac{a^2 + b^2}{R^2} \bar{\Omega}. \quad (6)$$

As in the Maclaurin case, the Jacobi sequence also reaches a secular instability, occurring at  $\bar{L}_{c2} = 0.395$ .

One should also note that an upper limit is imposed on the spin rate to avoid mass shedding, i.e. the ejection of particles situated on the equator of the body due to the centrifugal force locally overcoming gravity. For a sphere

$$\frac{\Omega_{\max}}{\sqrt{2\pi G\rho}} = \sqrt{\frac{2}{3}}. \quad (7)$$

In the case of an ellipsoids and considering a particle on the tip of an elongated three-axial body, this limit is lower. The corresponding formula have been derived, for example, by Richardson et al. (2005) and Harris (2002).

The systems of equations (2)–(6) show that the equilibrium solutions are defined in a four-dimensional parameter space. In the following we choose a description based on the two axis ratios ( $b/a, c/a$ ),  $\bar{\Omega}$  and  $\bar{L}$ . These four parameters will be used for analysis of the results, and they can be considered as independent since a generic shape, not

corresponding to a fluid equilibrium, will not satisfy the above mentioned relations. This four-variable set, anyway, is a first, practical approximation providing a description simple enough for a straightforward comparison to theory and observations.

Concerning the applicability of the equilibrium theory for fluids to bodies composed of solid fragments, Holsapple (2001) has shown that a more appropriate description is available in the frame of the Mohr–Coulomb theory, which can be applied to granular media. The most relevant parameter of this model is the critical angle (or angle of repose)  $\phi$ . For a pile of fragments of equal properties in a uniform gravity field (for example, a sand pile on the ground),  $\phi$  corresponds to the maximum sustainable slope of the pile. Richardson et al. (2005) have shown that the family of aggregates composed by spheres that are stable in the numerical model that we adopt satisfies the Mohr–Coulomb equilibrium for  $\phi \sim 40^\circ$ .<sup>2</sup> As a consequence, a large fraction of the parameter volume is populated with possible stable solutions (Section 4). In the following, we will check if those solutions are reachable by gravitational re-accumulation.

## 2.2. Observed shapes

In general, spin periods are derived from lightcurve data. Spin statistics seem to show that an upper barrier exists for the rotation rate of bodies above  $\sim 0.15$  km of diameter. Below  $\sim 10$  km this probably corresponds to the critical rotation above which the effect of centrifugal force would overcome a rubble-pile self-gravity (Pravec and Harris, 2000). For bodies larger than  $\sim 10$  km, the same effect is present, with the important difference that self-gravity alone could determine the critical threshold, being much stronger than the cohesion forces even in a compact, monolithic rocky structure (Holsapple, 2007). Rubble-pile structure for large bodies is thus possible, but cannot be inferred by the rotation barrier alone. Other data exist, however, supporting this hypothesis, such as the low bulk density measured for several asteroids, certainly related to a high porosity (Britt et al., 2002).

The richest existing collections of rotational pole coordinates and asteroid shapes are compiled using techniques of photometric inversion. Historically, shapes have been represented using ellipsoids or combinations of them (Magnusson, 1989; Farinella et al., 1981; Cellino et al., 1989), and only later more parameters were introduced in the inversion, in order to fit more features in the lightcurves. With modern inversion techniques, the asteroid convex hull has been described by a triangular mesh (Kaasalainen and Torppa, 2001; Kaasalainen et al., 2001). Incidentally, one should note that the inversion solution is not unique if concavities are taken into account.

<sup>2</sup>One can note that this angle is toward the upper limit for typical rock pile, usually in the  $20^\circ$ – $40^\circ$  range. This can depend upon the chosen particle shape and the related packing properties.

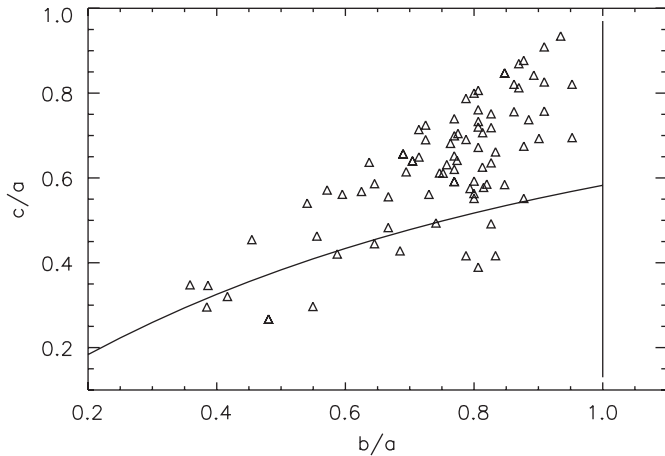


Fig. 1. Observed axis ratio from the Magnusson and Neese (1996) database. Only the objects having a value determined for both axes are shown. All of them are larger than  $\sim 10$  km in diameter. The vertical line on the right, corresponding to flattened spheroids ( $a = b$ ), represents the Maclaurin equilibrium solution, bifurcating into the Jacobi sequence (curved line) at the secular stability limit.

Another source of difficulty concerns the accuracy of the details of the mesh, which are hard to assess; however, the convex hull obtained by these techniques can be taken as representative of the overall shape.

In Fig. 1 we plot the axis ratios available from the asteroid spin vectors database (Magnusson and Neese, 1996). Only objects having both ratios determined are shown. A source of interpretation difficulty comes from the observational biases that can flaw the distribution. For example, the lack of asteroids close to the Maclaurin sequence ( $b/a \sim 1$ ) is due the difficulty of interpreting small amplitudes. In these cases the measurement of  $b/a$  is difficult, and that of  $c/a$  alone, requiring multi-opposition photometry, is rarely attempted.

The values are scattered considerably all over a large area of the axis ratio plane, without any appreciable clustering around the fluid stability curves. This fact does not allow us to draw any particular conclusion, since we do not know how many of the objects considered are rubble piles. Conversely, we know that even if they were, in general they would not behave as fluids (notably because of being able of sustaining shear strains).

### 2.3. Equilibrium shapes and satellites

The data above are presented as one planar projection of the four-dimensional parameter space introduced in Section 2.1. The construction of the other projections requires to know spin rate, mass and bulk density. This last parameter has only been determined with a good accuracy for an extremely reduced number of asteroids, due to uncertainties both in the mass (usually measured by mutual asteroid deflection) and in the absolute size (most often deduced from thermal infrared data).

However, in some cases, the determination of masses can be improved by the presence of a satellite, and sizes can be

measured by other methods, as it is being done by HST interferometry (Hestroffer et al., 2006). Asteroids visited by space probes constitute a limited but precious minority. If we use the available asteroid densities to study their distribution on the  $\bar{L}, \bar{\Omega}^2$  plane, it appears that a small group of asteroids seems to follow the Jacobi sequence. Surprisingly, they also possess a satellite (Hestroffer, 2004; Hestroffer and Tanga, 2005). For the ones whose secondary object is close in size to the primary, they accommodate along the Darwin sequence, describing shapes of binary objects (Descamps and Marchis, 2008).

It can be stressed that this particularity is not a result of a selection bias since the proportion of asteroids lying far from the fluid sequences—whatever their mass and angular momentum—is large, their shape not corresponding to fluid equilibrium states (as noted by Holsapple, 2001). As a consequence, it seems that the presence of a satellite plays a role in favoring fluid equilibrium shapes for the primary, and that a high angular momentum determines the preference for the Jacobi branch (Hestroffer and Tanga, 2005).

The origin of this fact could be related to: (i) seismic shaking or other tidally-induced flexures capable of bringing a cohesionless body to the fluid relaxed state; (ii) the re-accumulation process itself, after catastrophic collision of the parent asteroid. This second scenario further motivates a study of shape origin and evolution.

### 3. Numerical simulations: the approach

In this paper, we use `pkdgrav`, a parallel N-body code that uses a hierarchical tree structure to reduce the computational cost of force calculations. This is the same adopted in the shape stability study by Richardson et al. (2005). We recall here that the code is capable of solving collisions among hard spheres, and is thus suited for simulations in Solar System science.

Due to the organization of particles in a hierarchical tree, the computation speed is higher when particles have some clustering hierarchy in space. Of course, this is not the case of gravitational aggregates, for which most particles fill rather homogeneously the volume of the rubble pile. Also, their proximity results in a huge number of collisions to be detected and processed each time step. Simulations are thus extremely demanding in CPU and a wide exploration of the parameter space cannot be fruitfully done with more than  $\sim 1000$ – $2000$  particles, since several tens of simulations are needed.

For this study, we ran most of the simulations on a powerful cluster at the Observatoire de la Côte d'Azur (Nice, France). As in Richardson et al. (2005) we consider spheres of equal radius, with restitution coefficients 0.8 and 1.0 in the radial and tangential directions, respectively. We will present the results obtained in 50 runs, 30 with a number of particles  $N = 500$  and 20 with  $N = 1500$ , to check for a resolution dependency.

### 3.1. Initial conditions

Initially, particles are randomly dispersed in a cloud of ellipsoidal shape. The initial velocities are composed from two contributions. The first one is a component completely random and isotropic, whose modulus is uniformly extracted in an interval  $[0, v_{\max}]$ . A second component, providing a given amount of total angular momentum  $L$ , is then added. The numerical procedure ensures that the final velocities will stay below  $v_{\max}$ , i.e. that  $L$  is not due to very few particles each one carrying a lot of momentum but is indeed distributed in the whole particle set. Also,  $v_{\max}$  and  $L$  are chosen in such a way that the overall instability conditions for the cloud are met (self-gravitation potential energy wins over rotation and kinetic energy).

Due to the dissipation induced by the inelastic collisions the collapsing cloud will lose kinetic energy. The high collisional rate thus grants a rapid relaxation toward a dense body.

Of course, these initial conditions may sound simplistic. In the real world, gravitational collapse may be a highly chaotic process, conversely a uniformly populated ellipsoidal cloud of fragments can appear as a peculiar, highly ordered initial condition. Nevertheless this simplification is not far from the procedure introduced by D'Abramo et al. (1999) for establishing re-accumulation criteria based on kinetic energy and position of fragments when ejected from the parent body. In some conditions, this procedure identifies a domain of the parent body that remains gravitationally bounded without expanding during the disruption process. In the context of some simulations of family formation, this behavior is observed for the largest fragments (for example, the Eunomia parent body in Michel et al., 2002) that can form very rapidly from particles initially enclosed in a limited, fairly spherical volume. For these reasons, we assume that our initial conditions are not too unrealistic and—in any case—constitute a first reasonable approximation. Further studies will take advantage of having clarified the properties of this simple scenario for approaching more complex situations.

Again, we want to stress the main difference relative to Richardson et al. (2005): the fragments are initially dispersed in a cloud  $\sim 10$  times the size of the expected rubble pile, instead of being closely packed in pre-formed aggregates.

With the typical scaling for the simulated system (a cloud of fragments containing the mass of a 1 km asteroid, with particle density  $2 \text{ g cm}^{-3}$ ) the run duration corresponds to 40 h of evolution (physical time), implying 4000 steps of  $\sim 0.7$  min. This is longer than the typical duration for the accretion of the available mass (usually complete in  $\sim 10$  h) and ensures the stabilization of the accreted body.

### 3.2. Outcome analysis

The analysis of the re-accumulation outcome involves extracting the relevant parameters describing the body shape and spin properties.

The simulation records several outputs (position and velocity) at intermediate steps; an analysis program is run over all of them to verify that the relevant quantities have converged during the simulation.

The analysis program first isolates the re-accumulated body from possible fragments that have not fallen onto it. The resulting set of particles is then used to compute the body properties. The principal inertia axis are computed as the eigenvectors of the inertia matrix. The maximum distances of the particles from the aggregate center, projected onto the principal axis, provide the semi-axis lengths.

Once these elements are known, the derivations of spin axis direction, spin rate and angular momentum are straightforward. The final shape and rotation can then be represented by the adimensional parameters discussed in Section 2.1, independent from specific choices on particle mass and size.

Even if the analysis program offers an automated, fast procedure for extracting the physical parameters of interest, some possible hidden traps can sometime alter the meaning of the results.

First of all, the final aggregate is not always isolated from a dynamical point of view. In general, in fact, some non-reaccumulated fragments remain around it as single-particle satellites. Also, the collapse is not granted to produce a single object, but could well end up in two (or more?) re-accumulated masses, eventually orbiting around a common center. This fact has been observed and is of the greatest interest for studying satellite formation. Conversely, if the analysis code is run without ensuring that the nearby mass is not significantly perturbing the largest aggregate, the interpretation of the obtained parameters can be biased. The simulations have thus been carefully checked to rule-out such situations.

A second problem concerns the chosen scheme for shape representation. In fact, even a qualitative look to some gravitational aggregates we obtained shows a departure from ellipsoids, such as egg-like shapes. Since these anomalies appear to be small (i.e. of the same order of one particle diameter) we are confident that the results presented further on remain meaningful.

## 4. Results and discussion

The results obtained so far are summarized in the two plots of Fig. 2, each symbol representing the final outcome of a single run. For all the simulations presented here, the re-accumulated mass is more than 70% of the total, to grant an appropriate estimate of the shape and to avoid possible perturbations by satellitized particles, inducing tides and variable torques on the main aggregate.

The first interesting result is the tendency of the re-accumulated bodies to cluster around the fluid equilibrium curves. The simulations with  $N = 1500$  seem to come even closer to the curves, probably due to a better

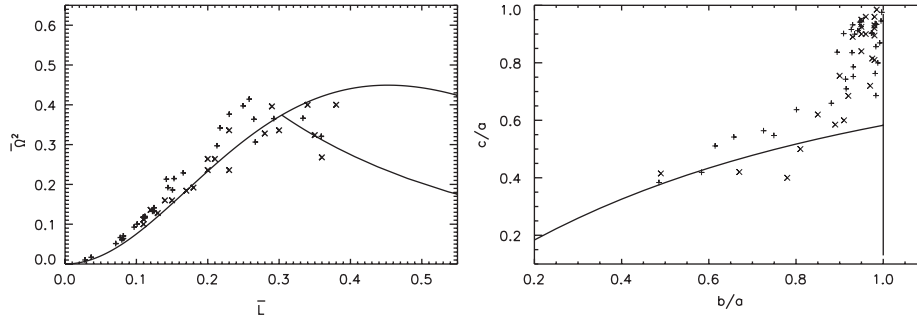


Fig. 2. Results of the simulation of the re-accumulation. Each symbol corresponds to the gravitational aggregate outcome of a single run. Values represented by + are for simulations with  $N = 500$  particles, while  $\times$  is for  $N = 1000$ . The right panel is similar to Fig. 1. The left panel is the  $\bar{L}, \bar{\Omega}^2$  projection. Here the Maclaurin sequence starts from the origin. After the bifurcation with the Jacobi branch (decreasing curve with positive concavity) the Maclaurin curve no longer corresponds to stable solutions.

approximation of the ellipsoidal shape. Despite several tests at high spin rates of the initial cloud, it appears very difficult to form aggregates with  $\bar{\Omega}^2 > 0.4$  since they are close to the mass-shedding limit for elongated ellipsoids. Also, if only the aggregates formed in an initially spherical cloud were considered, all the symbols close to the Jacobi branch ( $\bar{L} > \bar{L}_{c1}$ ) would disappear from the plot.

The only way to create Jacobi-like ellipsoids is to begin with very elongated three-axial clouds, for example, having  $a/c \sim b/c \sim 0.3$  or less. This “memory of the initial conditions” cannot probably be avoided with our approach. This can be heuristically understood by noting that, at a given value of  $\bar{\Omega}^2$ , moving to the Jacobi branch implies favoring a prolate ellipsoid relatively to the flattened spheroid, thus jumping to a higher  $\bar{L}$ . The main point here is that  $L$  is conserved all along the process: the final aggregate, containing almost all the mass, will also have about the same  $L$  than the initial cloud. Therefore, the only possibility to increase  $\bar{L}$  would be to re-accrete less mass (thus diminishing the normalization factor) but—on average—that would also lower  $L$ , due to the diminished contribution by the accreted fragments.

In other words, our experiments seem to indicate that a spherically symmetric collapse is not able to produce prolate ellipsoids but converge directly to a flattened spheroid. On the other hand, if an elongation of the particle cloud (with larger values of  $L$ ) is introduced in the initial conditions, it can be found also in the outcome under the form of aggregates that fall along the Jacobi branch at the highest  $\bar{L}$  values. We argue that this fact probably derives from the simple conservation of the angular momentum  $L$ , which is satisfied during the process due to the nearly complete re-accumulation of all fragments on the resulting final body.

More generally, the reason that the results fall close to the fluid equilibrium curves is not obvious.

This can be better understood by plotting the final, stable aggregates found by Richardson et al. (2005) with the same parametrization presented in this paper (Fig. 3). In the upper two panels, it is clear that a wide range of parameters is acceptable for the system, but this requires that the aggregates are pre-assembled. The theoretical limits that

hold are those deduced from the Mohr–Coulomb law and from the spin limit (see Richardson et al., 2005, for the full discussion).

The obtained distribution is very different from the one found as a result of our simulations (Fig. 2) although it could be compatible with the observed data (Fig. 1).

A selected fraction of the outcomes in Fig. 3 (upper panels) is plotted in the lower panels. These represent bodies undergoing a more or less dramatic restructuring with some mass loss. The original aggregates that generated them—initial conditions for the Richardson et al. (2005) simulations—were characterized, in general, by high values of  $\bar{\Omega}$  (above the Maclaurin–Jacobi bifurcation point). The mass loss and the relaxation to a new shape have brought the majority of them close to the fluid equilibrium curves.

The fact that the restructured bodies populate well the Jacobi branch on the left panel seems to confirm the arguments expressed above, since the simulations by Richardson et al. (2005) start always with  $b/a = c/a$ , thus not at spherical symmetry in the initial conditions. Also, the bodies falling on the Jacobi sequence loose in general a moderate amount of mass (they are identified with “ $\times$ ” on the plot). Bodies losing more mass (represented by “+”) are more scattered and the measurement of their final shapes is probably affected by the low number of remaining particles.

However, the convergence to the Jacobi sequence is only apparent on the left panel. The right panel shows that, in reality, the “ $\times$ ” aggregates remains fairly close to the  $b/a = c/a$  line where they were created. In fact, mass ejection essentially lowered  $\bar{\Omega}$ , but the shape was not allowed to change enough to reach the Jacobi sequence.

## 5. Conclusions and perspectives

We have shown here that aggregates composed by spheres can stably hold a large variety of shapes, but not all of them are reached with equal probability by a simple gravitational re-accumulation process. In other words, although the model admits several equilibrium solutions (Richardson et al., 2005), when there is a lot of energy to be

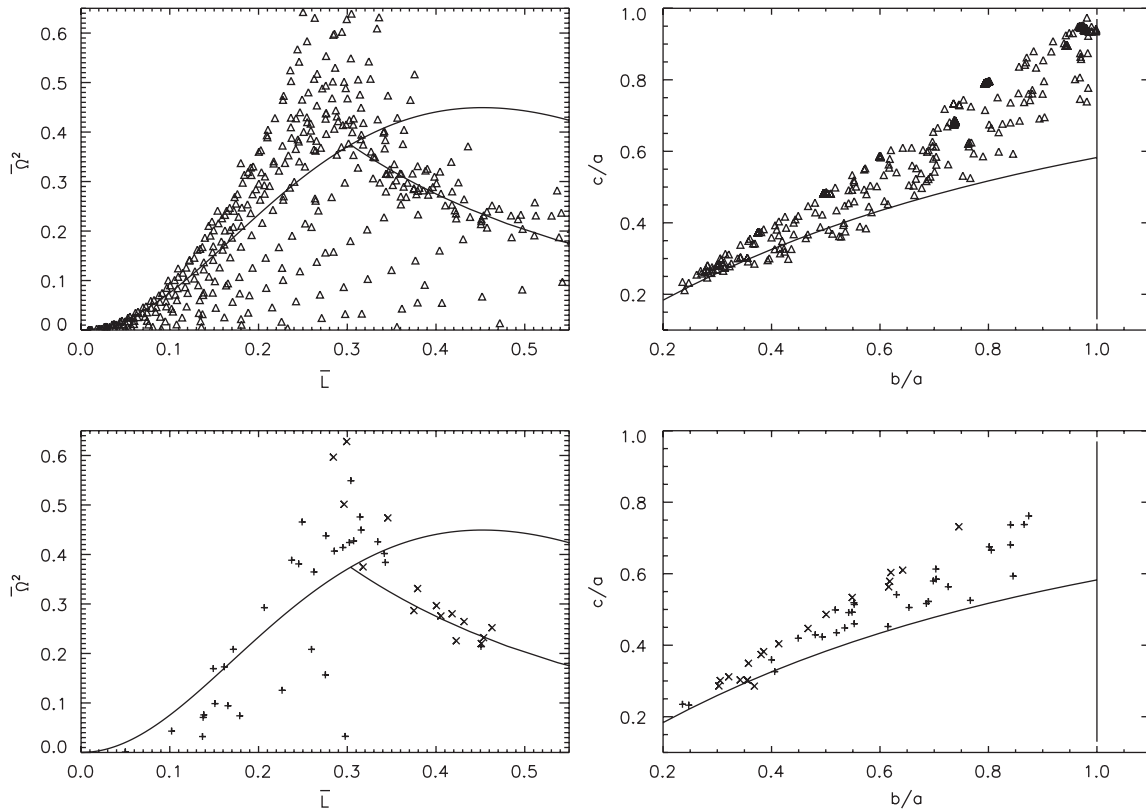


Fig. 3. Final, stable shape/spin states for the results obtained in Richardson et al. (2005), here re-plotted as a function of the same parameters as in Fig. 2. The top panels gather all the outcomes, while in the bottom panels only bodies that have been reshaped radically with non-negligible mass loss are plotted. Different symbols discriminate between different amounts of mass loss: 1–10% for  $\times$ ; and 10–50% for  $+$ .

dissipated, the resulting final shapes lie preferentially close to the equilibrium sequences for fluids.

The collapse process has also the tendency to preserve a memory of the initial conditions, i.e. of the shape of the initial cloud. The outcome of the inelastic collapse of dispersed fragments cannot thus be controlled simply by changing its spin. In particular, due to angular momentum conservation, an approximately spherical cloud of particles will preferentially generate axially symmetric spheroids on the Maclaurin sequence, while Jacobi ellipsoids will appear only for elongated clouds.

In all the simulations presented here, the whole process is very fast and most of the particles fall on the forming aggregate on a timescale shorter than the relaxation time of the aggregate itself. Although this behavior corresponds to what is observed in the fast formation of the largest remnants in the large re-accumulation simulations (Michel et al., 2001) other situations—such a slow, gradual buildup of particles—should be analyzed.

In any case, with a variety of initial conditions we are capable of producing ellipsoids lying anywhere on the Maclaurin stability line (and to some extent also on the Jacobi branch) but other stable solutions are *never* reached (for example, at intermediate values of  $\bar{\Omega}$  and  $\bar{L}$ ).

We thus cannot state here in a general way that the re-accumulation process is not capable of generating all the

shapes that are allowed by the Mohr–Coulomb law, but the strong tendency of aggregates to move toward the fluid equilibrium shapes seem to confirm that this last solution, representing a deeper energy minimum for these dynamical systems, is more probable. The most attractive region of the parameter space is certainly that of flattened spheroids on the Maclaurin sequence.

Concerning satellite formation, the only simulations efficiently producing secondary aggregates are those starting with very elongated, cigar-like clouds ( $c/a \sim b/a \sim 0.2$ ). In this situation, the cloud major axis is longer than the most unstable wavelength and the cloud separates into different portions before the re-accumulation phase, thus making the formation of multiple rubble piles easier. We will devote a future paper to satellite formation. Also, we plan to adopt a more general initial condition generator, since this is probably the key for obtaining an unbiased statistics.

Concerning the comparison with observations (Section 2.2), all we can say is that the pure re-accumulation, according to our findings, does not seem to generate directly the observed variety. Also, we have shown that the aggregates we generate close to the Maclaurin sequence can be accompanied by one or more satellites, consistently with the observations commented above (Section 2.3). This does not imply that asteroids with

satellite are unaltered examples of re-accumulated rubble piles. For example, tidal stresses induced by the satellite could be responsible for relocating material in the primary, bringing it closer to the fluid equilibrium sequence.

Another mechanism that could affect the observed rubble-pile shapes, include processes that change the object shape during its history, after its initial formation, such as non-disruptive impacts or YORP-induced spin accelerations. Eventually, further simulations should allow us to distinguish among the different mechanisms that generate a variety of rubble-pile shapes.

## Acknowledgments

We acknowledge the use of the *Mésocentre de calcul - SIGAMM* hosted at the Observatoire de la Côte d'Azur, Nice, France.

## References

- Britt, D.T., et al., 2002. Asteroid density, porosity, and structure. *Asteroids III*, pp. 485–500.
- Cellino, A., Zappalà, V., Farinella, P., 1989. Asteroid shapes and lightcurve morphology. *Icarus* 78, 298–310.
- Chandrasekhar, S., 1969. *Ellipsoidal Figures of Equilibrium*. Yale University Press, New Haven, CT.
- Consigli, J., Tanga, P., Hestroffer, D., Richardson, D.C., 2007. Asteroid shapes and satellite formation: role of gravitation reaccumulation. *C. R. Phys.* 8, 469–480.
- D'Abramo, G., Dell'Oro, A., Paolicchi, P., 1999. Gravitational effects after the impact disruption of a minor planet: geometrical properties and criteria for the reaccumulation. *Planet. Space Sci.* 47, 975–986.
- Davis, D.R., Chapman, C.R., Greenberg, R., Weidenschilling, S.J., Harris, A.W., 1979. Collisional evolution of asteroids: populations, rotations and velocities. In: *Asteroids*. University of Arizona Press, pp. 528–557.
- Descamps, P., Marchis, F., 2008. Angular momentum of binary asteroids: implications for their possible origin. *Icarus* 193, 74–84.
- Durda, D.D., Bottke, W.F., Enke, B.L., Merline, W.J., Asphaug, E., Richardson, D.C., Leinhardt, Z.M., 2004. The formation of asteroid satellites in large impacts: results from numerical simulations. *Icarus* 170, 243–257.
- Farinella, P., Paolicchi, P., Tedesco, E.F., Zappalà, V., 1981. Triaxial equilibrium ellipsoids among the asteroids. *Icarus* 46, 114–123.
- Farinella, P., Paolicchi, P., Zappalà, V., 1982. The asteroids as outcomes of catastrophic collisions. *Icarus* 52, 409–433.
- Hachisu, I., Eriguchi, Y., 1984. Fission sequence and equilibrium models of rigidity rotating polytropes. *Astrophys. Space Sci.* 99, 71–74.
- Harris, A.W., 2002. On the slow rotation of asteroids. *Icarus* 156, 184–190.
- Hestroffer, D., Tanga, P., 2005. Figures of equilibrium among binary asteroids. *Bull. Am. Astron. Soc.* 37, 1562.
- Hestroffer, D., et al., 2006. HST/FGS high angular resolution observations of binary asteroids. *Bull. Am. Astron. Soc.* 38, 615.
- Hestroffer, D.J.G.J., 2004. On equilibrium shapes among binary asteroids. *Bull. Am. Astron. Soc.* 36, 861.
- Holsapple, K.A., 2001. Equilibrium configurations of solid cohesionless bodies. *Icarus* 154, 432–448.
- Holsapple, K.A., 2007. Equilibrium configurations of solid cohesionless bodies. *Icarus* 154, 432–448.
- Kaasalainen, M., Torppa, J., 2001. Optimization methods for asteroid lightcurve inversion. I. Shape determination. *Icarus* 153, 24–36.
- Kaasalainen, M., Torppa, J., Muinonen, K., 2001. Optimization methods for asteroid lightcurve inversion. II. The complete inverse problem. *Icarus* 153, 37–51.
- Lai, D., Rasio, F.A., Shapiro, S.L., 1993. Ellipsoidal figures of equilibrium—compressible models. *Astrophys. J. Suppl.* 88, 205–252.
- Magnusson, P., 1989. Pole determinations of asteroids. In: *Asteroids II*. University of Arizona Press.
- Magnusson, P., Neese, C. (Eds.), 1996. *Asteroid Spin Vectors*. EAR-A-5-DDR-ASTEROID-SPIN-VECTORS-V4.2. NASA Planetary Data System.
- Michel, P., Benz, W., Tanga, P., Richardson, D.C., 2001. Collisions and gravitational reaccumulation: forming asteroid families and satellites. *Science* 294 (5547), 1696–1700.
- Michel, P., et al., 2002. Formation of asteroid families by catastrophic disruption: simulations with fragmentation and gravitational reaccumulation. *Icarus* 160, 10–23.
- Pravec, P., Harris, A.W., 2000. Fast and slow rotation of asteroids. *Icarus* 148, 12–20.
- Richardson, D.C., Elankumaran, P., Sanderson, R.E., 2005. Numerical experiments with rubble piles: equilibrium shapes and spins. *Icarus* 173, 349–361.
- Tanga, P., Consigli, J.F., Hestroffer, D., Comito, C., Cellino, A., Richardson, D.C., 2006. Are asteroid shapes compatible with gravitational reaccumulation? *Bull. Am. Astron. Soc.* 38, 615.
- Yeomans, D.K., et al., 1997. Estimating the mass of asteroid 253 Mathilde from tracking data during the NEAR Flyby. *Science* 278, 2106.